Effects of Morphology and Surface Characteristics of Poly(imide siloxane)s and Deep UV/O_3 Surface Treatment on the Interfacial Adhesion of Poly(imide siloxane) / Alloy-42 Leadframe Joints

Shyi-Liang Jwo[1], Wha-Tzong Whang[1,*], Tsung-Eong Hsieh[1], Fu-Ming Pan[2], and Wen-Chang Liaw[3]

1. *Department of Materials Science and Engineering, National Chiao Tung University, HsinChu 300, Taiwan, Republic of China*
2. *National Nano Device Laboratory, 1001-1 Ta Hsueh Rd., HsinChu 30050, Taiwan, R.O.C.*
3. *Department of Chemical Engineering, National Yunlin University of Science and Technology, 123, Section 3, Ta Hsueh Road, Touliu, Yunlin 640, Taiwan, R.O.C.*

Abstract: The effect of surface characteristics and morphology of poly(imide siloxane) (PIS) on the true interfacial adhesion between PIS films and alloy-42 substrates was studied. The effect of the viscosity of PIS films and the surface treatment of deep UV/O_3 (d-UV/O_3) on alloy-42 plates on the peel strength of PIS films/alloy-42 joints has also investigated. 3,3',4,4'-benzophenone tetracarboxylic dianhydride/2,2'-bis[4-(3-aminophenoxy)phenyl]sulfone (BTDA/*m*-BAPS) based PIS films with α,ω-bis(3-aminopropyl)polydimethyl siloxane (APPS) molecular weight M_n = 996 g/mole (PIS9Siy) show two phases in all compositions and the linear dependence of the critical surface tension on the surface concentration of the silicon, [Si_{surf}], on the PIS films. The PIS films with the APPS M_n = 507 g/mole (PIS5Siy) or M_n = 715 g/mole (PIS7Siy) exhibit a morphology change from a homogeneous phase to an inhomogeneous phase starting at the mole ratio (y) of APPS/PIS = 2.7% and 1.1%, respectively. The curves of critical surface tension dependence on the [Si_{surf}] discontinue or deflect at these two compositions, respectively. The treatment of d-UV/O_3 on alloy-42 plates improves the wetting on the alloy surface and promotes the peel strength between the PIS films and alloy-42 plates by a magnitude of ≥ 20%. These results show that the flowability of the same PIS films bonding at different temperatures significantly affects the bonding strength of the joints, but the flowability of different PIS films bonding at the same temperature, e.g. 400 °C, is not the key factor governing the bonding strength of the joints. The true interfacial adhesion of the PIS5Si0.6/alloy-42 joint is 80% higher than that of the unmodified BTDA/*m*-BAPS based polyimide film/alloy-42 joint. However, zero true interfacial adhesion is obtained between the PIS9Siy films and alloy-42 plates. The wetting kinetics experiment shows that the higher the siloxane content in the PIS, the higher the activation energy for the adhesive bonding process. Moreover, the phase sepration significantly increases the activation energy. The scanning electron micrographs of the peeled-off PIS film surfaces from the PIS/alloy-42 joints reveal the rougher surface morphology from the sample with the higher interfacial adhesion.

Keywords: Poly(imide siloxane) film, True interfacial adhesion, Morphology, Critical surface tension, Phase separation, Alloy-42 leadframe, Peel strength.

*To whom all correspondence should be addressed.
Tel: 886-3-5731873; Fax: 886-3-5724727
E-mail: sachen.@che.nthu.edu.tw

J. Polym. Res. is covered in ISI (CD, D, MS, Q, RC, S), CA, EI, and Polymer Contents.

Introduction

Polyimides, being thermally stable and mechanically tough, have been widely utilized in the electronic and microelectronic industries [1-4] and aerospace fields [5-7]. Polyimides are usually modified with siloxane segments to confer low moisture absorption [4] and high qualify interfacial adhesion on the polyimide/substrate interface [4,8-12]. Siloxane modified polyimides, called poly(imide siloxane)s, (PISs), are block copolymers consisting of imide and siloxane blocks. In the memory device package using Lead-on-Chip (LOC) technology, the leadframe (metal) is laminated on the top of the integrated circuit (IC) chip with a double sided adhesive tape (e.g. a poly(imide siloxane) tape) by a hot press process taking several seconds. The reliability of the interfacial adhesion between the PIS film and the substrate is crucial. It has been shown that the adhesive strengths of the polymers are related to their surface properties (e.g. critical surface tension) [13]. L. H. Lee [14] proposed that the critical surface tension of a copolymer is related to the mole fraction and the critical surface tension of each homopolymer. In most of the interfacial adhesion studies of polyimides or PIS on various substrates, the polyimide films were usually applied either from poly(amic acid) solution onto the substrates and cured at elevated temperatures [3,10,15-18] or applied via chemical vapor deposition [19]. However, in the LOC package, the polyimide standing film is directly laminated on the lead frame substrate under pressure and heat in a short time. The interfacial adhesion is mainly dependent on the adsorption of the metallic substrate surface with the polyimide adhesive by means of adsorption adhesion [20]. The surface tension and the wettability of the polyimide film to the substrate are critical in adhesion behavior.

For LOC applications, the polyimides are modified with siloxanes to improve the interfacial adhesion with the metallic substrates. Because of the difference in the solubility parameters between the aromatic imide blocks and the siloxane imide blocks in the PIS, the incorporation of different contents and molecular weights of the siloxane segment can cause a change in the morphologies of the PIS film, e.g. in the phase separation [21]. In turn, it may change the adhesive strength of the PIS on the substrate. In general, siloxanes due to low surface energy are known as release agents. Their relatively low surface energy causes the siloxane segments to migrate to the polymer surface with relative ease [9, 15]. It is well known that surface composition plays an important role in the wettability of the surface. Moreover the flowability of the polymer film may affect the interfacial adhesion of the film/substrate joint. However, a systematic study of the correlation of the interfacial adhesion of the PIS/alloy-42 leadframe joints with the morphology, the surface characteristics and the high temperature flowability of the PIS film is not available. In this study, a series of poly(imide siloxane)s were prepared from BTDA, *m*-BAPS and APPS with various APPS contents and three APPS molecular weights to study the effect of the composition and morphology, wettability and flowability of the PIS film on the interfacial adhesion of PIS/alloy-42 joints. In addition, a simple procedure called a d-UV/O_3 process is carried out to improve the interfacial adhesion by treating the surface of the leadframe metal in air with a deep UV light (λ = 172 nm), which can generate ozone molecules that work together with the deep UV light to clean the surface. Each of the PIS films is directly hot-pressed onto an alloy-42 substrate in several seconds. The adhesion strength is measured using a self-designed peel tester, while the surface tension and composition are measured using a surface tension testing device and an X-ray photoelectron spectroscope (XPS), respectively. The glass transition temperature and the mechanical properties are studied with a dynamic mechanical analyzer (DMA), the peeled-off surface morphologies are determined with a scanning electron microscope (SEM), and the viscosity (or the flowability) is measured with a rheometric dynamic spectrometer.

Experimental

1. Materials and their purification

High purity octamethylcyclotetrasiloxane (D4, purity > 97%), 1,3-bis(3-amino-propyl)-1,1,3,3-tetramethyldisiloxane (DSX, purity > 97%) from United Chemical Technologies and tetramethylammonium hydroxide pentahydrate (purity > 98%) from Lancaster Synthesis Ltd. were used in synthesis without further purification. BTDA (Aldrich Co.) was purified by recrystallization from acetic anhydride (purity: 99.8%, Tedia Co.) and then dried in a vacuum oven at 120 °C for at least 14 hours. High purity (99.23%) *m*-BAPS (Chriskev Co.) was subjected to a thermal treatment in a vacuum oven at 90 °C for 3 hours prior to use. *N*-Methyl-2-pyrrolidone (NMP, Tedia Co.) was dried over molecular sieves. The leadframe material was an alloy-42 plate, an alloy of nickel and iron, available from Sitron Precision Co., Ltd.

2. Synthesis of APPS oligomers

A catalyst for tetramethylammonium siloxanolate (TMAS) was prepared from 4.31 g (0.0233 moles) of tetramethylammonium hydroxide

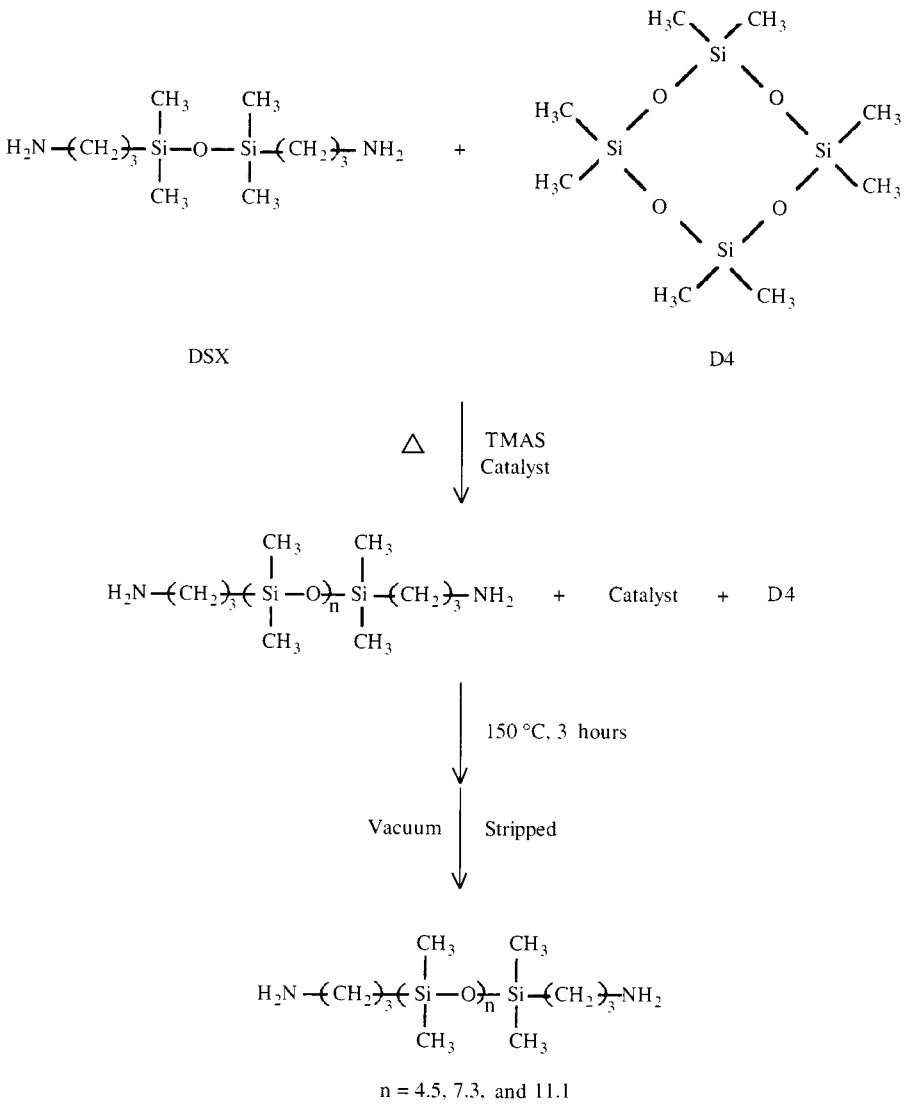

Scheme 1.

pentahydrate and 32.11 g (0.1050 moles) of D4 in a 3-neck flask with magnetic stirring at 62~66 °C under a strong argon stream for about 48 hours [22-24]. The argon stream was bubbled through the reaction solution to remove the water completely. After the completion of the dehydration, a viscous translucent siloxanolate catalyst was obtained and stored in a refrigerator before the synthesis of APPS oligomers.

Three APPS oligomers were synthesized using an equilibration polymerization method [22,25,26] involving DSX and D4 in the presence of the siloxanolate catalyst. The reactions are shown in Scheme 1.

Three APPS oligomers were synthesized with molecular weights equal to 507, 715, and 996 g/mole, respectively, and corresponding to n = 4.5, 7.3, and 11.1, respectively. The APPS oligomer of molecular weight 507 g/mole was prepared by first heating the mixture of 8.42 g (0.0339 moles) of DSX along with 4.99 g (0.0168 moles) of D4 to 80 °C in a flask with a nitrogen stream, and then adding 0.13 g (~1.0 wt%) of tetramethylammonium siloxanolate catalyst into the mixture. The reaction was conducted at 80 °C for 48 hours, and then raised to 150 °C for 3 hours to decompose the catalyst. After cooling, the mixture was vacuum (~0.1 torr) stripped at about 105 °C for 4 hours to remove the residual D4. The number average molecular weight, $\overline{M}_n$, determined by means of the proton nuclear magnetic resonance (^{1}H NMR) spectroscopy [25], was 507 g/mole. Similarly, the APPS oligomers of molecular weights 715 g/mole and 996 g/mole were synthesized by the same method with the appropriate mole ratio of DSX/D4 and with the same weight percent of the catalyst in the reaction and their molecular

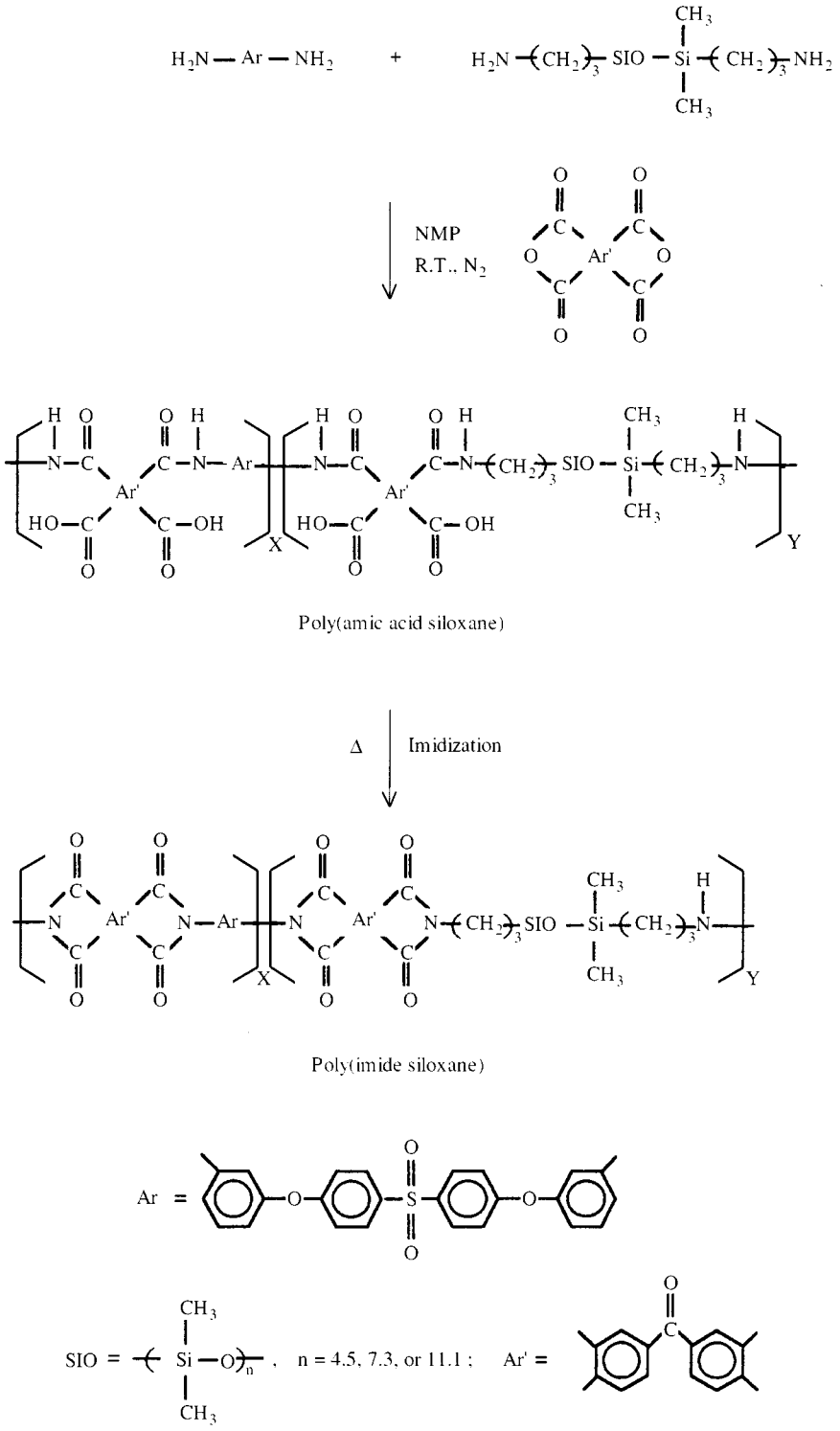

Scheme 2.

weights were also characterized with the proton NMR.

3. Sample preparation

A series of polyimides were prepared from BTDA, *m*-BAPS and APPS ($\overline{M}_n$ = 507, 715 and 996 g/mole, respectively). The reaction is shown in Scheme 2. The percentages of the mole ratios of APPS to poly(imide siloxane), APPS/PIS, were 0, 0.4, 0.6, 1.1, 1.7, 2.7, 7.7, 10.0, 13.7, 16.6, 19.0, 49.7, and the mole ratio of the total diamines to the dianhydride for the reactions was kept at 1/1.01. The

moles of PIS are defined as the total mole number of the dianhydrides and the diamines. The PIS with the APPS/PIS mole ratio of 49.7 was prepared from APPS and BTDA (1/1.01 mole ratio), but no *m*-BAPS.

The poly(imide siloxane)s made from APPS with the molecular weight of 507, 715, and 996 g/mole, respectively, were encoded as PIS5Siy, PIS7Siy, and PIS9Siy, respectively, with the "y" value standing for the percentage of the mole ratio of APPS/PIS.

A three neck 100 mL round bottom flask was fitted with a mechanical stirrer, a nitrogen inlet, and a gas outlet. The flask was first purged with nitrogen gas and heated on a hot plate to remove the moisture. Then, the flask was cooled down to the ambient temperature under a nitrogen stream.

In a typical reaction to prepare PIS5Si0.6, 1.6110 g of BTDA (0.0050 moles) was added into the solution containing 2.1279 g of *m*-BAPS (0.00492 moles), 0.0414 g of APPS (0.00008 moles) and 10.7528 g of dry NMP. BTDA was introduced into the solution in five portions an hour apart. The poly(amic acid siloxane), (PAAS), solution was then stored in a freezer (at about -15 °C). Polymerizations were conducted at a solid content (w/w) of 26%.

For critical surface tension and surface composition measurements, the poly(amic acid siloxane) was spin-coated on a clean glass slide and then imidized in a vacuum oven at temperatures of 100, 150, 200, 250 and 300 °C, each for 1 hour. The samples were placed in clean glass containers with lids, then stored at 23 ± 3 °C and 55 ± 5% R.H. in a dry box before testing.

For thermal or mechanical properties testing, the PAAS solution was coated on a PET sheet with a thickness of 250 μm. The PAAS was then heated at 100 °C for 1 hour in a forced air convection oven to remove the solvent. The PAAS film was then transferred to a rectangle stainless frame clamp and imidized at temperatures of 150, 200, 250 and 300 °C, each for 1 hour. The film thickness was 28 ± 2 μm. Other PIS films were also prepared in a range of thicknesses from 7 to 62 μm for peel strength measurement.

Similarly, the films of other poly(imide siloxane)s with different mole ratios of APPS/PIS and different molecular weights of APPS were also prepared by the same method.

Peel test specimens were prepared by pressing directly the sample PIS film onto the alloy-42 plate using the following processes. (1) The alloy-42 plate (40 mm × 25 mm × 0.2 mm) was first cleaned with degreasing solution (5 wt%, Galtin 212) at 50 °C for 5 minutes and then ultrasonically cleaned in deionic water and acetone. It was then dried in a nitrogen stream and in an oven at 160 °C for 10 minutes. (2) The PIS film or the alloy-42 plate was treated with a deep UV/O_3 source (wavelength 172 nm, 200 W, Xe_2^* excimer Model: UER20, USHIO, Inc.). The distance of irradiation was 8.0 mm, and irradiation time was 0, 0.6, 1, 2, 3, 5, 7, or 10 minutes. (3) The alloy-42 plate was put on a hot plate at a controlled temperature and the PIS sample film (25 mm × 5 mm) was suspended over the 42-alloy plate at a distance of ~5 mm at the ambient temperature of 150 °C for 8 minutes, followed by applying a load of 3~13 Kg/cm^2 for 2~10 seconds. It was then stored in a desiccator for peel strength measurement.

4. Measurement and characterization

The morphology and phase behavior of the PIS films were studied with an Olympus BHSM polarizing optical microscope and a SEM. The details have been described in our previous paper [21].

A series of homologous surface tension standard solutions (Sherman Treaters Ltd., U. K., mixtures of 2-ethoxyethanol formamide and methylene blue dye), with surface tensions of 58, 50, 40, 35, 31 dyne/cm, were used in the critical surface tension measurements of the PIS films. The surface tensions of the standard solutions were double-checked by the Fisher autotensiomat (model : KIOST) at 22 ± 1 °C and 55 ± 5% R.H. the precision of the surface tension values was less than -0.5 dyne/cm. The contact angles of the PIS films (supported upon a clean glass slide) with the standard solution were measured by the equilibrium sessile-drop method using a goniometer (model 100-00, Rame-Hart, Inc.). The measurements were carried out at 22 ± 1 °C and 55 ± 5% R.H. in an air-conditioned room. At least three drops (1.5~2.0 mm diameter, prepared with a microsyringe) of each solution on the surface of the sample films were observed. Equilibrium contact angles were measured on both sides of each drop within 25 seconds. The errors were less than 5%.

The critical surface tension of the sample was evaluated by the Zisman's linear approximation method [20,27]. A curve regression was used to fit a straight line to the points using a computer program (Sigma plot program).

Similarly, the contact angles of the surface of the cleansed alloy-42 plate and the glass slide with deionic water were measured by the same method. The surface was treated with the d-UV/O_3 device at an irradiation distance of 8.0 mm before measurement. The irradiation time was 0, 20, 40, 60, or 120 seconds. Glass transition temperatures of the aromatic imide blocks of the poly(imide

Table I. The glass transition temperatures of the BTDA/*m*-BAPS imide block and tensile moduli of poly(imide siloxane)s from a dynamic mechanical analyzer, and the microscopic observation of the poly(imide siloxane)s.

Sample code / Properties / APPS/PIS mole ratio (%, "y")	PIS5Siy			PIS7Siy			PIS9Siy		
	T_g[a] (°C)	Tensile modulus (Gpa)	Phase separation	T_g[a] (°C)	Tensile modulus (Gpa)	Phase separation	T_g[a] (°C)	Tensile modulus (Gpa)	Phase separation
0	252	3.29 ± 0.09	H[b]	252	3.29 ± 0.10	H	252	3.29 ± 0.10	H
0.4	--[c]	--	--	--	--	--	244	2.83 ± 0.11	PS[e]
0.6	251	3.21 ± 0.10	H	2 44	3.05 ± 0.11	H	244	2.81 ± 0.12	PS
1.1	245	3.12 ± 0.11	H	244	3.00 ± 0.13	PS	243	2.69 ± 0.12	PS
1.7	241	3.00 ± 0.11	H	242	2.93 ± 0.13	PS	241	2.47 ± 0.13	PS
2.7	238	2.78 ± 0.13	PS	240	2.50 ± 0.14	PS	239	2.30 ± 0.14	PS
7.7	224	2.35 ± 0.14	PS	231	2.03 ± 0.13	PS	233	1.77 ± 0.16	SPC[e]
10.0	--	--	PS	229	1.74 ± 0.15	SPC	--	--	--
16.6	195	1.84 ± 0.16	SPC	--	--	--	--	--	--

(a) The glass transition temperature of the aromatic BTDA/*m*-BAPS imide block, and the standard deviation for the T_g is less than ±1 °C.
(b) A homogeneous phase.
(c) Not determined.
(d) Two phase, one siloxane-rich phase dispersed in BTDA/*m*-BAPS rich phase.
(e) The siloxane-rich phase becomes a continuous phase.

siloxane)s were determined using a TA Instruments DMA 2980 dynamic mechanical analyzer at a heating rate of 2 °C/min from 45 to 300 °C. The samples (15 mm × 5 mm) were run at a frequency of 1 Hz with a film tension clamp. The peak temperature in tanδ was chosen as the T_g. At least three specimens were tested. Stress-strain tests were also performed on the same equipment using the TMA Controlled Force mode. The PIS samples (20 mm × 4 mm) were elongated at a ramp force of 4 N/min at room temperature. At least five specimens were tested. The dynamic viscosities of the PISs were measured with a rheometric dynamic spectrometer (model: RDS-7700, Rheometrics, Inc.) from 250 to 400 °C at a heating rate of 2 °C/min. A VG Microlab Mark III scanning Auger microscope equipped with a 150 °C sector energy analyzer was used to perform X-ray photoelectron spectroscopy measurements of the surface concentration of the silicon in the PIS films. The base pressure of the system was below 1×10^{-10} Torr. The X-ray source was mainly the Mg K_α line (1253.6 eV) produced at 15 KV and 20 mA. The take-off angle and the pass energy used in the XPS measurements were 90° and 50 eV, respectively. The peel strength was measured on a self-designed peel tester (model HT-8116, Hung TA Instrument Co., Ltd.). The tester was constructed with a special design sample holder to maintain a 90° peel angle. The peel strength was measured using a 4 Kg load cell with 8×10^{-3} Kg resolution and was transmitted to a personal computer for data processing. The measured peel strength was averaged when the force reached a steady state. The hot-pressed PIS films were cut into 2~3 mm wide strips with a sharp knife. The peel strength of the film/substrate joint was measured at the peel rate of 10 mm/min. At least four specimens were tested. The peeled-off PIS film surface from PIS/alloy-42 joints was examined using a Hitachi S-4000 scanning electron microscope after prior vapor deposition of a thin gold film.

Results and Discussion

All the BTDA/*m*-BAPS based poly(imide siloxane)s can be cast to form flexible free standing films. Their thermal characteristics and morphologies have been presented in our previous paper [21]. In this paper we aimed to study the effect of bonding conditions of the PIS films onto the alloy-42 substrate and the effect of their surface characteristics, morphology, and flowability on the adhesion strength in order to design a better PIS film for the LOC package. In the LOC packaging process, low bonding temperatures are desirable, yet they must be high enough to render the best possible adhesive strength. Usually, temperatures are in the range of T_g+100 to T_g+150 °C and should not exceed 400 °C. The dynamic mechanical analysis data in Table I show the glass transition temperatures (T_g) of the aromatic imide block in the range of 195 to 251 °C; the tensile moduli decrease with the mole ratio of APPS to PIS and with the APPS molecular weight. The results of microscopic morphology of the PIS films are also shown in Table I. Phase separation begins at PIS5Si2.7 for the PIS5Siy series, at PIS7Si1.1 for the PIS7Siy series. In the PIS9Siy series, the phase separation appears even at a very low siloxane content (y = 0.4%). The siloxane-rich phase disperses in the BTDA/*m*-BAPS aro-

Table II. XPS analysis of poly(imide siloxane)s film surface.

Sample code / Properties: APPS/PIS mole ratio (%, "y")	PIS5Siy			PIS7Siy			PIS9Siy		
	$[Si_{bulk}]^{(a)}$ (%)	$[Si_{surf}]^{(b)}$ (%)	$R^{(c)}$	$[Si_{bulk}]^{(a)}$ (%)	$[Si_{surf}]^{(b)}$ (%)	$R^{(c)}$	$[Si_{bulk}]^{(a)}$ (%)	$[Si_{surf}]^{(b)}$ (%)	$R^{(c)}$
0.6	0.11	6.0 ± 0.4	54.5	0.18	8.1 ± 0.8	45.0	0.27	9.1 ± 0.6	33.7
1.1	0.20	7.3 ± 0.9	36.5	0.33	9.2 ± 0.9	27.9	0.49	10.2 ± 0.7	20.8
1.7	0.31	8.1 ± 0.8	26.1	0.51	9.2 ± 0.7	18.0	--[d]	--	--
2.7	0.49	9.4 ± 0.7	19.2	--	--	--	1.20	12.0 ± 0.8	10.0
7.7	1.47	10.1 ± 0.6	6.9	2.27	11.5 ± 0.4	5.1	3.26	15.5 ± 0.3	4.8
10.0	--	--	--	2.93	12.1 ± 0.4	4.1	4.16	15.8 ± 0.5	3.8
13.7	--	--	--	3.97	12.3 ± 0.8	3.1	--	--	--
16.6	3.21	11.2 ± 1.0	3.5	--	--	--	--	--	--
19.0	3.70	11.2 ± 0.8	3.0	--	--	--	--	--	--
Pure BTDA/APPS, PSI[e]	10.1	13.8 ± 1.0	1.4	13.1	16.1 ± 1.0	1.2	15.5	19.9 ± 1.2	1.3

(a) Calculated.
(b) Surface.
(c) $R = [Si_{surf}]/[Si_{bulk}]$.
(d) Not determined.
(e) The pristine BTDA/APPS poly(siloxane imide) (PSI).

matic imide rich phase. The siloxane phase becomes a continuous phase as the mole ratio of APPS/PIS reaches 7.7%, 10.0%, and 16.6% in PIS9Siy, PIS7Siy, and PIS5Siy, respectively.

The surface concentrations of silicon on the PIS films from the theoretical calculation of the bulk, $[Si_{bulk}]$, and the XPS analysis, $[Si_{surf}]$, are listed in Table II. It is observed that the surface concentrations of silicon $[Si_{surf}]$ on all the PIS films are much higher than the corresponding bulk concentrations $[Si_{bulk}]$. It is well known that the surface energy of a solid sample can reach the lowest value at an equilibrium state. Because of the relatively low surface energy (or critical surface tension) of BTDA/APPS poly(siloxane imide) in comparison with that of the pure BTDA/*m*-BAPS polyimide (unmodified polyimide) as shown in Table III, APPS tends to migrate to the surface, where it produces a low energy surface. As shown in Table II, $[Si_{surf}]$ increases with the content and the molecular weight of APPS in the PIS films before the siloxane imide block becomes a continuous phase. The $[Si_{surf}]$ does not further change as the mole ratio of APPS/PIS reaches ≥ 7.7%, 10.0%, and 16.6% in PIS9Siy, PIS7Siy, and PIS5Siy, respectively. This may be attributed to the siloxane imide blocks for a continuous phase, as reported in our previous paper [21], in the PIS matrix as the mole ratio of APPS/PIS ≥ 7.7%, 10.0% and 16.6% for PIS9Siy, PIS7Siy, and PIS5Siy, respectively. However, the ratios of $[Si_{surf}]$ to $[Si_{bulk}]$ decrease with the APPS content and the molecular weight of APPS in the PIS films. Because the surface energy of the BTDA/APPS siloxane imide block decreases with the APPS molecular weight, more of the APPS segment should migrate to the surface during heating to make the surface energy as low as possible if the PIS has a lower APPS content or a shorter APPS segment. The pristine BTDA/APPS poly(siloxane imide)s have the ratios of $[Si_{surf}]/[Si_{bulk}]$ in the range of 1.2 to 1.4. This means that even in the pure pristine poly(siloxane imide), the surface concentration of silicon is slightly greater than the bulk concentration.

Table III. Critical surface tensions (r_c, dyne/cm) of poly(imide siloxane)s[a].

APPS/PIS mole ratio (%, "y")	PIS5Siy	PIS7Siy	PIS9Siy
0	32.2	32.2	32.2
0.6	23.6	22.0	20.6
1.1	23.0	21.7	20.4
1.7	22.6	21.7	20.3
2.7	22.6	21.6	20.1
7.7	22.3	21.1	19.8
10.0	--[b]	20.8	19.8
13.7	--	20.8	--
16.6	21.6	--	--
19.0	21.6	--	--
Pure BTDA/APPS, PSI[c]	20.9	20.4	19.7

(a) Errors are less than 5%.
(b) Not determined.
(c) The pristine BTDA/APPS poly(siloxane imide) (PSI).

The critical surface tensions (γ_c) of BTDA/*m*-BAPS based poly(imide siloxane) films are listed in Table III. Note that a significant decrease in the critical surface tension is observed between the pristine BTDA/*m*-BAPS polyimide and the PIS films, even at low APPS content. The γ_c values are in the range of 23.6~21.6, 22.0~20.8 and 20.6~19.8 dyne/cm for the films PIS5Siy, PIS7Siy, and

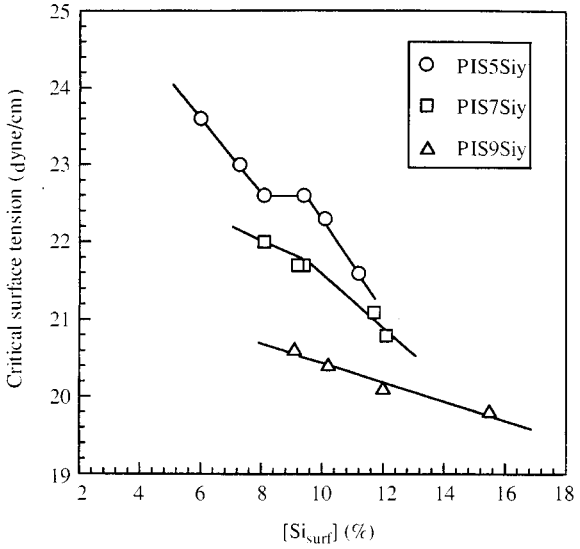

Figure 1. The dependence of the critical surface tension on the surface concentration of silicon of the PIS films (o) PIS5Siy, (❑) PIS7Siy, and (Δ) PIS9Siy.

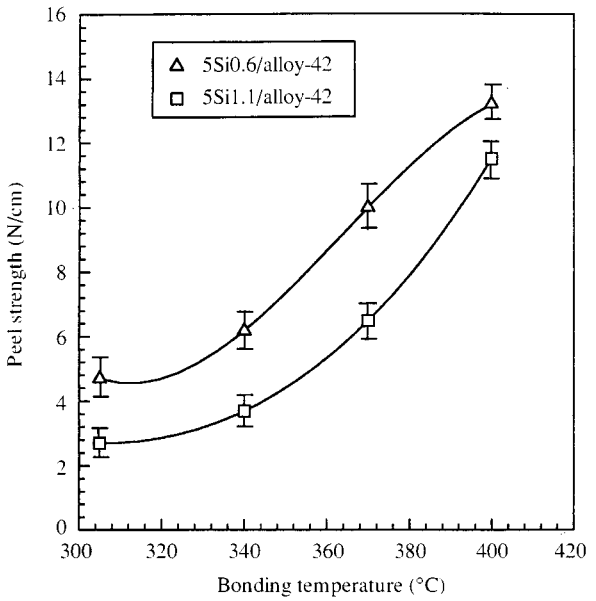

Figure 2. Effect of the bonding temperature on the peel strength between the PIS film and alloy-42 at a constant pressure of 6 Kg/cm^2 and bonding time of 2 seconds.

PIS9Siy, respectively. The γ_c of the PIS film decreases with the content and the molecular weight of APPS. According to L. H. Lee's proposal [14], the critical surface tension of a copolymer is related to the mole fraction and the critical surface tension of each homopolymer. The critical surface tension of the film is governed by the composition of the surface layer. In turn, the composition of the surface layer affects the interfacial adhesion of the film with the other substrate, here, the alloy-42 plate. We will discuss this effect in the following section. The dependence of the critical surface tension on the surface concentration of silicon [Si$_{surf}$] in the PIS films is shown in Figure 1. In PIS5Siy films, the critical surface tension is inversely proportional to the surface concentration of silicon, but there is a discontinuity at γ_c = 22.6 dyne/cm at which the morphology changes from homogeneity to inhomogeneity. In PIS7Siy films, the linear curve of γ_c versus [Si$_{surf}$] deflects at γ_c = 21.7 dyne/cm, where phase separation begins. In PIS9Siy films, the γ_c is linearly dependent on the [Si$_{surf}$] in all tested compositions, all in two phase morphology (inhomogeneous morphology).

The peel strength between the PIS films and the alloy-42 substrate, and the peeled-off PIS surface are studied to explore the effect of the APPS on the interfacial adhesion. The surface of the alloy-42 substrate is first cleansed before bonding with the designated process. In addition, the substrate surface is further treated with d-UV/O_3, which has been used to improve the surface wetting of cleansed ITO glass in liquid crystal display (LCD) manufacture. The deep UV light can decompose the oxygen molecule O_2 to form oxygen atoms, which, in turn, combine with oxygen molecules to form ozone molecules. The deep UV light and ozone molecules work together to cleanse the glass surface by a specific chemical reaction which decomposes the adsorbed organic monolayer and improves the surface wetting. The data of Table IV show that the d-UV/O_3 treatment significantly improved the surface wetting of the alloy-42 plates and the slide glass within one minute. After twenty seconds the contact angle of water on the alloy-42 substrate decreased from 32° to 4°, and down further to 0° after one minute. On the glass slide surface, the water contact angle decreased from 33° to 6° after 20 seconds, and down further to 0° after one minute.

Figure 2 shows the dependence of the peel strength of the PIS5Si0.6/alloy-42 and the PIS5Si1.1/alloy-42 interface on the bonding temperature. The peel strength increases dramatically with the bonding temperature: the higher the bonding temperature, the higher the peel strength. This result may be due to the higher flowability of the same PIS film at the higher temperature. Figures 3 and 4 show the peel strength between the PIS5Si0.6/alloy-42 and the PIS5Si1.1/alloy-42 interface as a function of the bonding pressure and time, respectively. It is found that a bonding pressure of no less than 6 Kg/cm^2 is required to obtain an optimum peel strength. The peel strength does not change if the bonding time is in the range of 2~10 seconds. To compare PIS films with different contents and molecular weights of APPS, in this study,

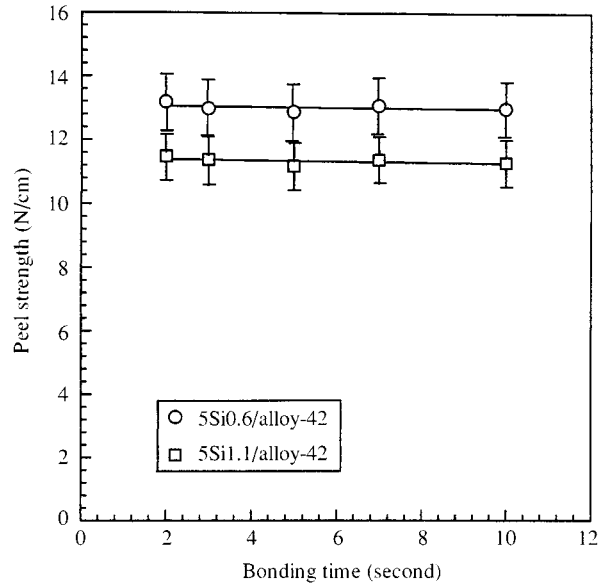

Figure 3. Effect of the bonding time on the peel strength between the PIS film and alloy-42 at a constant temperature of 400 °C and pressure of 6 Kg/cm^2.

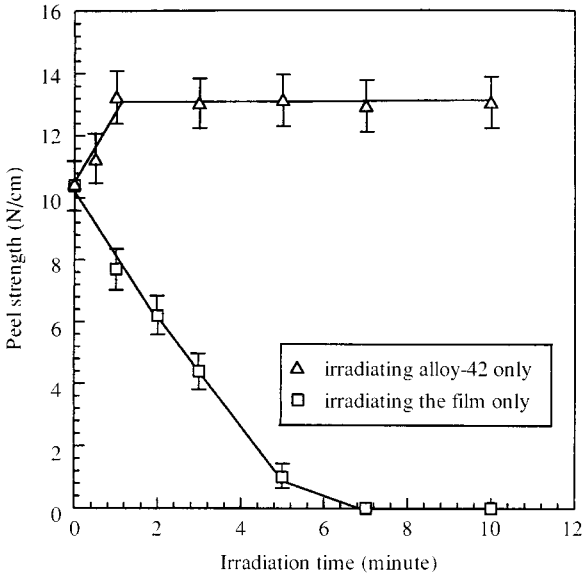

Figure 5. Effect of the time of irradiation with d-UV/O_3 on the peel strength between the PIS5Si0.6 film and alloy-42 substrate by treating the film and substrate separately.

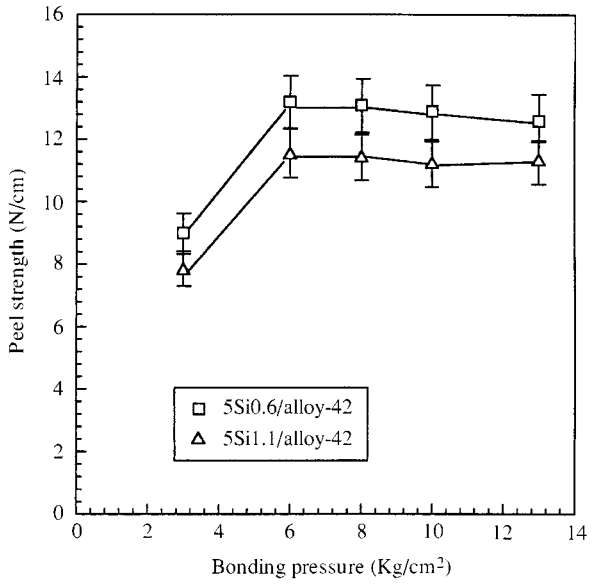

Figure 4. Effect of the bonding pressure on the peel strength between the PIS film and alloy-42 at a constant temperature of 400 °C and bonding time of 2 seconds.

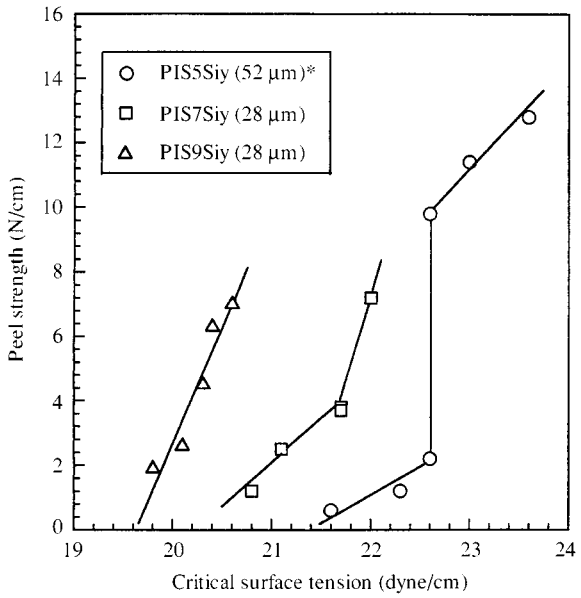

Figure 6. The dependence of the peel strength of the PIS film/alloy-42 joint on the critical surface tension of the PIS films at a bonding temperature of T_g+150 °C. (*film thickness).

the bonding condition for all the PIS films was measured performed at a temperature of 400 °C or T_g+150 °C with a pressure of 6 Kg/cm^2 for 2 seconds.

Figure 5 shows the effect of the d-UV/O_3 irradiation on the peel strength of the PIS5Si0.6/alloy-42 joint. It is found that irradiating the alloy-42 substrate with d-UV/O_3 for one minute can improve the peel strength to a magnitude of ≥ 20%, but irradiating the PIS film degrades the peel strength significantly. The data in Table V further confirm that an increase of at least 20% in the peel strength of all the tested PIS5Siy/alloy-42 joints can be achieved by irradiating the alloy-42 plate for just one minute, a really simple way to improve the peel strength.

The dependence of the peel strength of the PIS/alloy-42 joints on the critical surface tension is shown in Figure 6. For PIS5Siy films, the peel

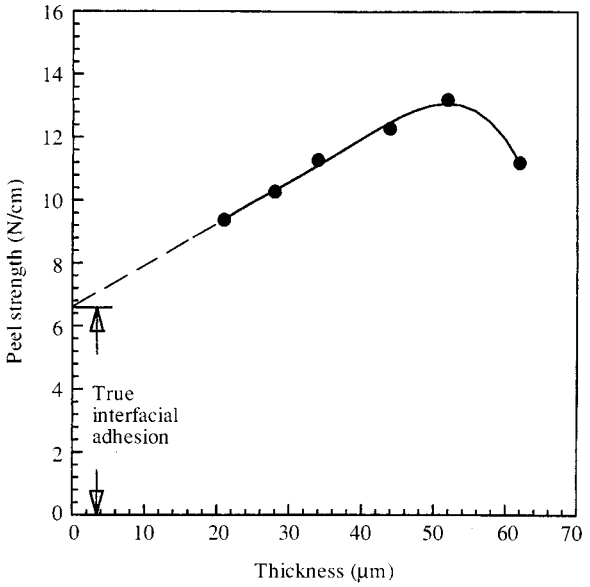

Figure 7. The measurement of the true interfacial adhesion between the PIS5Si0.6 film and alloy-42 from the dependence of the peel strength on the film thickness.

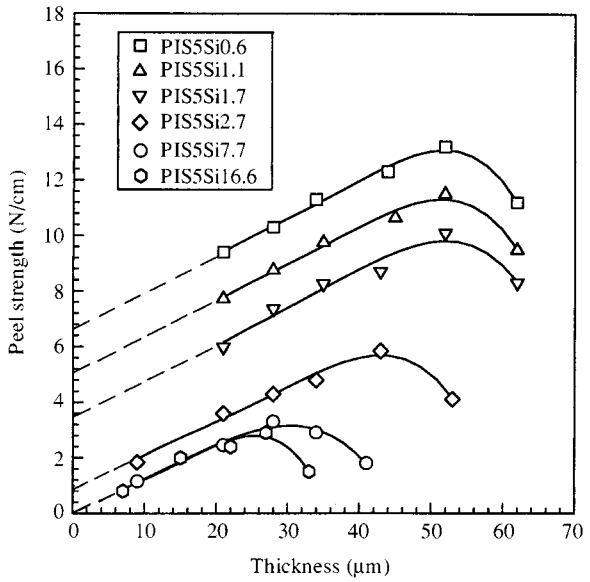

Figure 8. The measurement of the true interfacial adhesion between the PIS5Siy films and alloy-42 from the dependence of the peel strength on the film thickness.

strength is linearly proportional to the critical surface tension (γ_c) but displays a discontinuity at γ_c = 22.6 dyne/cm, where/at which point the morphology changes from homogeneity to inhomogeneity. The slopes of the upper linear curve and lower curve are different. In PIS7Siy systems, the linear dependence of peel strength on the critical surface tension deflects at γ_c = 21.7 dyne/cm, at which point two-phase morphology appears instead of homogeneous

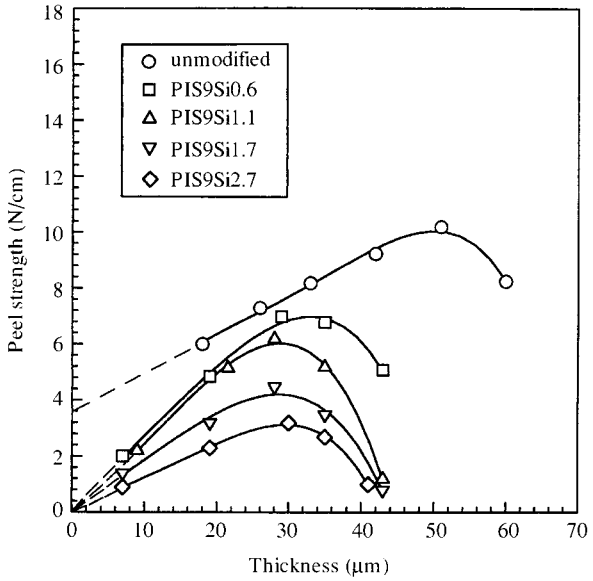

Figure 9. The measurement of the true interfacial adhesion between the PIS films and alloy-42 from the dependence of the peel strength on the film thickness.

Table IV. Changes in water contact angles upon exposure to d-UV/O_3 for alloy-42 or slide glass substrate.

Substrate	Exposure time (sec)	Water contact angle (°)[a]
Alloy-42	0	32
Alloy-42	20	4
Alloy-42	40	3
Alloy-42	60	0
Alloy-42	120	0
Slide glass	0	33
Slide glass	20	6
Slide glass	40	5
Slide glass	60	0
Slide glass	120	0

(a) Errors are less than 5%.

Table V. Effect of the d-UV/O_3 treatment on the peel strength of PIS film/alloy-42 substrate joints at a bonding temperature of T_g+150 °C.

Property / Sample code[a]	Peel strength (N/cm) Untreated	Treated[b]
5Si0.6	10.4 ± 0.6	12.8 ± 0.7
5Si1.1	9.4 ± 0.5	11.4 ± 0.5
5Si1.7	8.1 ± 0.7	9.8 ± 0.5
5Si2.7	1.8 ± 0.2	2.2 ± 0.2
5Si7.7	1.0 ± 0.1	1.2 ± 0.1
5Si16.6	0.5 ± 0.1	0.6 ± 0.1

(a) The film thickness is 52±2 μm.
(b) The alloy-42 substrate is additionally treated with d-UV/O_3 for 1 minute.

TableVI. The peel strength and true interfacial adhesion of PIS films/alloy-42 joints at a bonding temperature of 400 °C.

Characteristics / Strength (N/cm) / Sample code	Thickness (μm)							True interfacia adhesion (N/cm)
	8 ± 1	20 ± 2	28 ± 2	34 ± 1	43 ± 2	52 ± 2	62 ± 1	
Unmodified	C.B.P.[a]	6.0 ± 0.5	7.3 ± 0.6	8.2 ± 0.7	9.2 ± 0.6	9.9 ± 0.6	8.2 ± 0.7	3.6
5Si0.6	C.B.P.	9.0 ± 0.5	9.9 ± 0.5	10.9 ± 0.6	12.2 ± 0.8	13.2 ± 0.7	10.9 ± 0.6	6.6
5Si1.1	C.B.P.	7.8 ± 0.7	8.7 ± 0.6	9.6 ± 0.5	10.6 ± 0.7	11.5 ± 0.6	9.3 ± 0.5	5.1
5Si1.7	C.B.P.	5.9 ± 0.5	7.2 ± 0.6	7.8 ± 0.7	8.6 ± 0.7	9.9 ± 0.5	8.1 ± 0.6	3.5
5Si2.7	1.8 ± 0.2	3.3 ± 0.3	4.1 ± 0.4	4.5 ± 0.4	5.8 ± 0.6	3.6 ± 0.3	--[b]	0.9
5Si7.7	1.1 ± 0.2	2.5 ± 0.4	3.3 ± 0.3	2.9 ± 0.3	1.8 ± 0.3	1.2 ± 0.3	--	0
5Si16.6[c]	1.0 ± 0.2	2.4 ± 0.3	2.9 ± 0.4	1.5 ± 0.3	0.9 ± 0.2	0.6 ± 0.1	--	0
9Si0.6	2.2 ± 0.2	5.0 ± 0.4	7.0 ± 0.6	6.8 ± 0.6	4.9 ± 0.4	1.1 ± 0.2	--	0
9Si1.1	2.2 ± 0.2	5.3 ± 0.4	6.4 ± 0.4	4.8 ± 0.4	1.0 ± 0.2	--	--	0
9Si1.7	1.4 ± 0.1	3.2 ± 0.3	4.7 ± 0.4	3.2 ± 0.4	0.8 ± 0.1	--	--	0
9Si2.7	0.9 ± 0.2	2.4 ± 0.3	3.0 ± 0.5	2.6 ± 0.3	0.8 ± 0.2	--	--	0

(a) The PIS film cracked before peeling (C.B.P.) from the alloy-42 plate.
(b) Not determined.
(c) The peel strength was 1.9±0.2 N/cm for the film thickness of 15 μm.

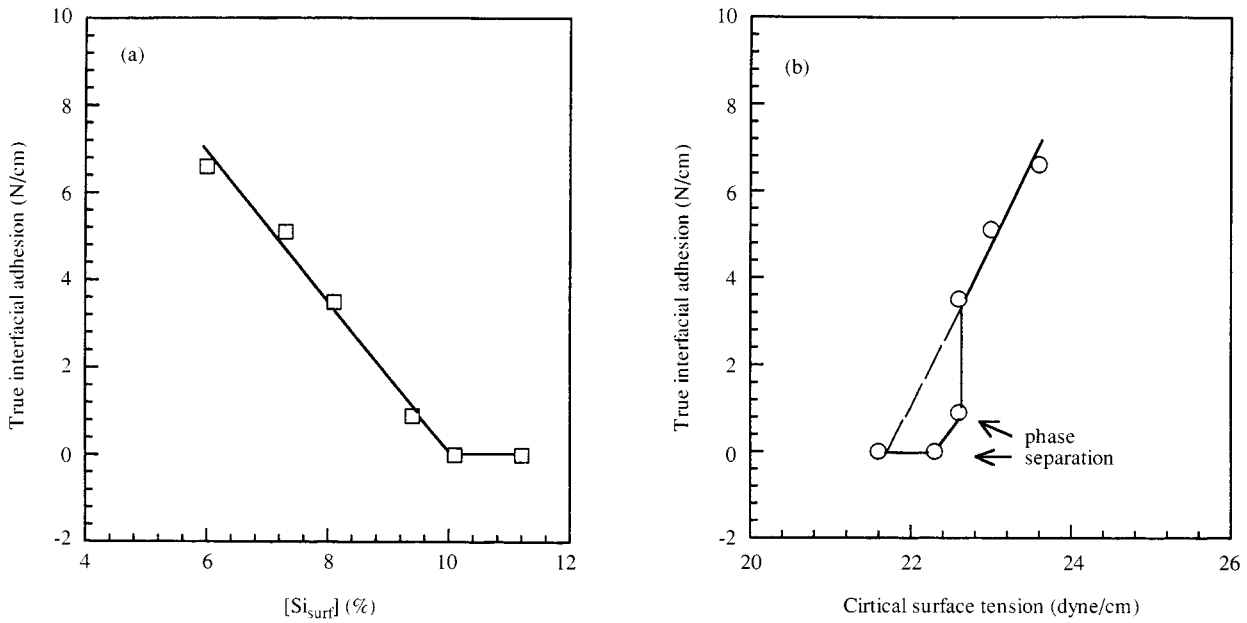

Figure 10. The dependence of the true interfacial adhesion of PIS5Siy/alloy-42 joint on (a) the surface concentration of silicon and (b) the critical surface tension of the PIS films.

morphology. For PIS9Siy films with two-phase morphology in all tested compositions, the peel strength is linearly proportional to the critical surface tension without any discontinuity or deflection point. Apparently, the morphology of the PIS films affects the behavior of the peel strength of the PIS/alloy-42 joints. The interface adhesion behavior of two different types of PIS film-PIS5Siy and PIS9Siy-on alloy-42 plates is further discussed in the following section.

The peel strength of the PIS/alloy-42 and the unmodified polyimide (PI)/alloy-42 plate joints is PIS or PI film thickness dependent, as shown in Figures 7~9 and Table VI. The peel strength of these joints consists of the true interfacial adhesion (i.e., decohesive strength of the interface, or the peel force per unit width in the absence of plastic deformation) between the films and the alloy-42 plate and the force for plastic deformation of the films during peeling [28-33]. According to Gent and Hamed [29], true interfacial adhesion can be obtained by extrapolating the curve of the peel strength dependence on the film thickness to zero thickness, as shown in Figure 7. The plastic deformation contribution to the peel strength can be obtained by subtracting the true interfacial adhesion from the peel

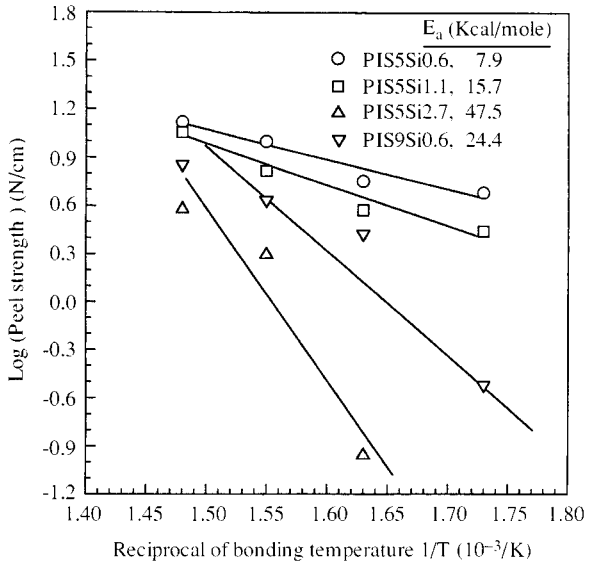

Figure 11. The peel strength between the PIS films and alloy-42 as a function of the reciprocal of bonding temperature.

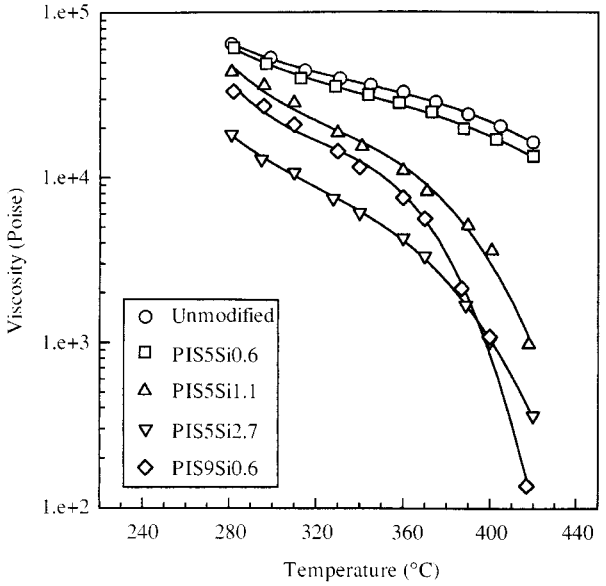

Figure 12. Viscosity as a function of temperature for poly(imide siloxane)s.

strength. Figures 8 and 9 show the curves of the peel strength dependence on the film thickness for the PIS5Siy and PIS9Siy(also for unmodified PI), respectively. It is found (also shown in Table VI) that the incorporation of low content and low Mn of siloxane in the PI improves the true interfacial adhesion of PIS/alloy-42 joints. For PIS5Si0.6, the improvement is 80% higher than that of the unmodified PI/alloy-42 joint. However, the higher the siloxane content, the lower the maximum peel strength for both PIS systems. The dependence of the true interfacial adhesion of the PIS5Siy/alloy-42 joints is inversely proportional to the surface concentration of silicon on the PIS films, as shown in Figure 10(a). The true interfacial adhesion becomes zero after $[Si_{surf}] > 9.4\%$ (that is, PIS5Si2.7). Figure 10(b) shows the true interfacial adhesion linearly proportional to the critical surface tension when the PIS5Siy film is homogeneous at low siloxane content. However, the true interfacial adhesion drops rapidly when two phase morphology appears in the PIS films, beginning at PIS5Si2.7. As shown in TableVI, the true interfacial adhesion of PIS9Siy/alloy-42 joints is zero in all compositions of the PIS films. This result may be related to the two-phase morphology of the PIS films in all tested compositions in which the siloxane segments act as release agents. Two different types of PIS films exhibit different behaviors with regard to the true interfacial adhesion. The activation energy for the bonding process can be calculated from the dependence of the peel strength of the PIS5Siy/alloy-42 and the PIS9Si0.6/alloy-42 joints on the reciprocal of bonding temperatures as shown in Figure 11. According to the wetting kinetics of bond formation [13]

$$\sigma_f = \sigma_f^o \exp(-E_a / RT) \quad (1)$$

where σ_f is the adhesive bond strength at time t, σ_f^o that at time zero, E_a the activation energy for the adhesive bonding process (wetting activation energy), R the gas constant, and T the bonding temperature (K). The E_a's of PIS5Si0.6, PIS5Si1.1 and PIS5Si2.7 on alloy-42 are 7.9, 15.7, and 47.5 Kcal/mole, respectively. PIS5Si2.7 has a much higher activation energy in the adhesive bonding process than the other homologue. It is found that in the same series of PIS films, phase separation leads to a much higher wetting activation energy. The activation energy of PIS9Si0.6 is 24.4 Kcal/mole, higher than those of PIS5Si0.6 and PIS5Si1.1, but lower than that of PIS5Si2.7.

Figure 12 shows the dependence of the viscosity of the PIS films on the temperature. The viscosity of the film is related to the flowability under bonding pressure. The higher the viscosity, the lower the flowability. Usually, the higher flowability favors the diffusion process of the films in the bonding process. If the diffusion is one of the controlled factors in the bonding process, the flowability of the PIS may affect the bonding strength. The viscosity at 400 °C follows the order: PIS5Si0.6 > PIS5Si1.1 > PIS5Si2.7~PIS9Si0.6. Generally speaking, the lower the viscosity, the faster the diffusion process. But true interfacial adhesion also follows the same order: PIS5Si0.6 > PIS5Si1.1 > PIS5Si2.7 > PIS9Si0.6. Therefore, the flow ability of the films at the bonding temperature is not the

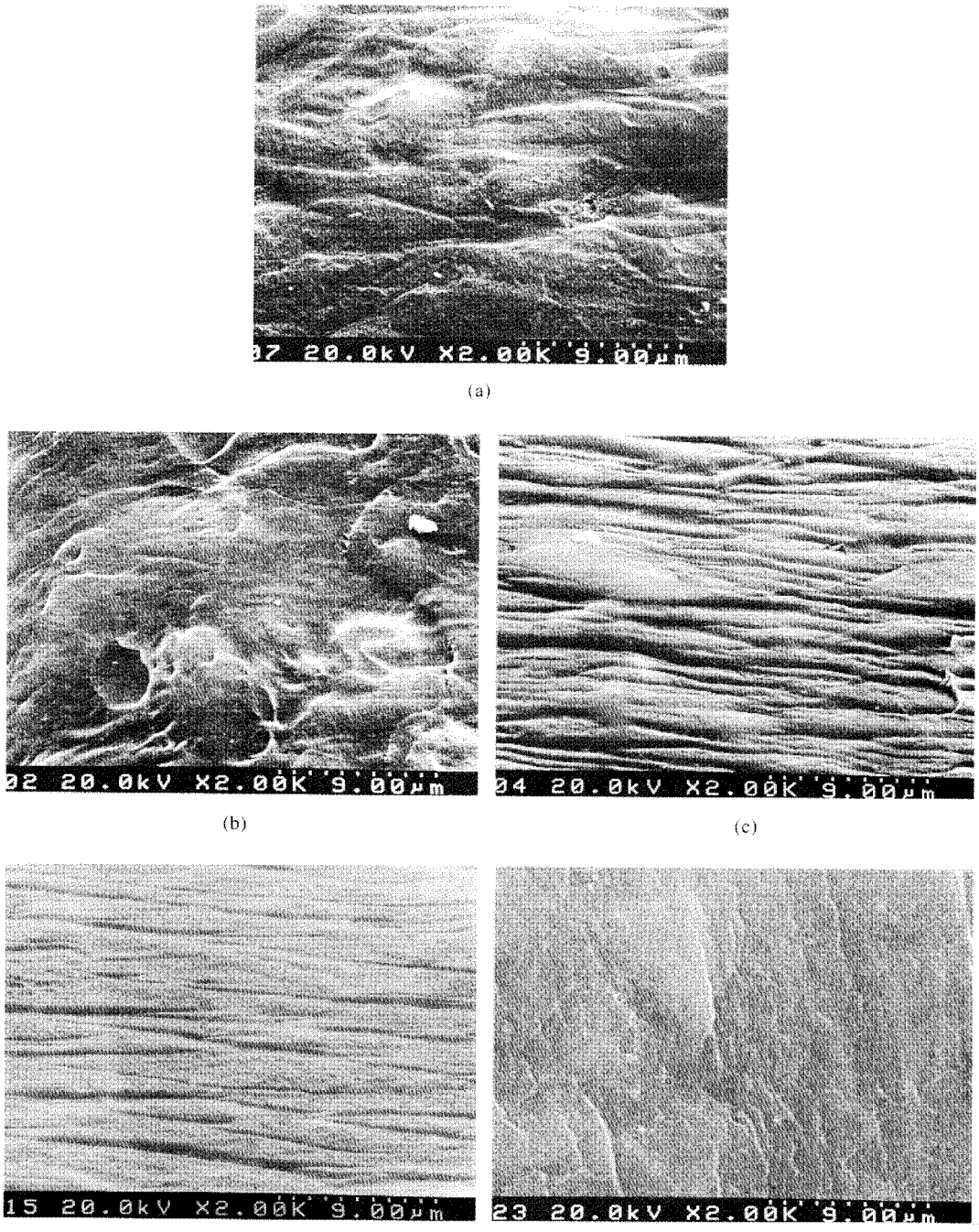

(a)

(b)

(c)

(d)

(e)

Figure 13. Scanning electron micrographs of the peeled-off PIS film surface from PIS film/alloy-42 joints at a 10 mm/min peel rate: (a) without d-UV/O_3 treatment to alloy-42 plate for PIS5Si0.6, and (b)~(e) treating UV/O_3 to alloy-42 for (b) PIS5Si0.6, (c) PIS5Si1.1, (d) PIS5Si2.7, and (e) PIS9Si0.6.

key factor governing the bonding strength of the PIS/alloy-42 joints.

The SEM micrographs of the peeled-off PIS surfaces can be used to explore the fracture mechanism. The SEM micrographs of the peeled-off PIS surfaces are shown in Figure 13. Figure 13(a) shows the peeled-off surface of the PIS5Si0.6 film on the surface of alloy-42 without d-UV/O_3 treatment. Comparing Figure 13(a) with the surface morphology of PIS5Si0.6 film on d-UV/O_3-treated alloy-42 shown in Figure 13(b), it is evident that treating the alloy-42 plate with d-UV/O_3 leads to a more extensive roughness of the PIS film bonded on the alloy-42 plate. The effects of the composition of the PIS films on the extent of roughness of the peeled-off PIS surfaces are shown in Figures 13(b)

~13(e). The extent of the roughness follows the order: PIS5Si0.6 > PIS5Si1.1 > PIS5Si2.7 > PIS9Si0.6, the same order as that for true interfacial adhesion, meaning that higher interfacial adhesion makes the PIS film harder to peel off from the alloy-42 plate. Therefore, greater force is needed to peel it off and more energy is consumed to pull the polymer chain of the PIS film from the alloy-42 plate. Hence, rougher surface morphology is observed on the higher interfacial adhesion PIS films.

PIS9Si0.6/alloy-42 joints with zero true interfacial adhesion have a peel strength higher than PIS5Si2.7/alloy-42 joints with a true interfacial adhesion of 0.9 N/cm, but the peeled-off surface from the former joint is smoother than that from the latter. It is reasonable to deduce that the peel strength of PIS9Si0.6/alloy-42 joints is due to the force of plastic deformation.

On the other hand, the locus of the failure of PIS film/alloy-42 joints was observed by the naked eye during the peel test. The film was broken, not peeled off, from the alloy-42 substrate during the peel test, when the $[Si_{surf}] \leq (6.0 \pm 0.4)\%$ for PIS5Siy films. The break was in the PIS5Siy film (e.g. PIS5Si0.6) and was not due to interface delamination, indicating that the strength of the interfacial adhesion was greater than that of the PIS film. However, PIS5Siy/alloy-42 joint delaminates at the PIS5Siy/alloy-42 interface as the PIS5Siy film (e.g. PIS5Si1.1) with the $[Si_{surf}] \geq (7.3 \pm 0.9)\%$. Similarly, PIS7Siy/alloy-42 and PIS9Siy/alloy-42 joints, when $[Si_{surf}] \geq (8.1 \pm 0.8)\%$ for all tested PIS films, also peeled from the interface.

Conclusions

The surface characteristics and the morphology of the BTDA/*m*-BAPS based PIS films affect the true interfacial adhesion between PIS films and alloy-42 substrates. The surface concentration of silicon $[Si_{surf}]$ on the PIS film is much higher than the bulk concentration $[Si_{bulk}]$. The $[Si_{surf}]$ increases with the content and the molecular weight of APPS in the PIS films. However, the ratio of $[Si_{surf}]$ to $[Si_{bulk}]$ decreases with the APPS content and the molecular weight of APPS in the PIS films. The critical surface tension of the PIS film decreases with the content and the molecular weight of APPS. The surface tension is also a function of the $[Si_{surf}]$ and the morphology of the PIS films. In either homogeneous or inhomogeneous morphology, the critical surface tension is inversely proportional to the surface concentration of silicon, but the linearity becomes discontinuous or deflects as the morphology changes from homogeneity to inhomogeneity. PIS5Siy and PIS7Siy films exhibit the morphology change from homogeneous phase to inhomogeneous phase beginning at PIS5Si2.7 and PIS7Si1.1, respectively. PIS9Siy films show two phases morphology in all the film series and linear dependence of the γ_c on the $[Si_{surf}]$. The linear dependence of the peel strength of the PIS/alloy-42 joints on the critical surface tension also shows the same morphology effect as mentioned above. The morphology of the PIS films significantly affects the behavior of the peel strength between the PIS films and the alloy-42 substrates.

The peel strength of PIS5Si0.6/alloy-42 joints strongly depends on the bonding temperature, and may be due to the lower viscosity and higher flowability of the film at the bonding temperature. The surface treatment of the alloy-42 substrate with d-UV/O_3 for one minute can improve the wetting of the alloy surface and promote the peel strength between the PIS film and the alloy-42 plate to a magnitude of at least 20%. The viscosities of the PIS films at 400 °C follow the order: PIS5Si0.6 > PIS5Si1.1 > PIS5Si2.7~PIS9Si0.6, and the true interfacial adhesion of these films also follows the same order. Therefore, the flowability of different PIS films at the bonding temperature of 400 °C is not the key factor governing the bonding process of the PIS/alloy-42 joints. The incorporation of siloxane in the polyimide indeed improves the true interfacial adhesion of PIS/alloy-42 joints. For PIS5Si0.6, the improvement is 80% higher than that of the unmodified BTDA/*m*-BAPS based polyimide/alloy-42 joints. However, the higher the content and the molecular weight of siloxane, the lower the maximum peel strength for the PIS series. The true interfacial adhesion of PIS9Siy/alloy-42 joints is zero in all compositions of the PIS9Siy films. This result may be related to the two-phase morphology of the PIS films. The true interfacial adhesion of PIS5Siy is inversely proportional to the surface concentration of silicon and becomes zero after $[Si_{surf}] > 9.4\%$ (that is, PIS5Si2.7). The adhesion is linearly proportional to the critical surface tension as the PIS5Siy film is homogeneous at low siloxane content. But the true interfacial adhesion decreases rapidly as two-phase morphology appears in the PIS films, starting at PIS5Si2.7.

The activation energy for the bonding process of PIS5Siy/alloy-42 and the PIS9Si0.6/alloy-42 joints can be calculated according to the wetting kinetics of bond formation. The activation energies of PIS5Si0.6, PIS5Si1.1, PIS5Si2.7 and PIS9Si0.6 films on alloy-42 are 7.9, 15.7, 47.5 and 24.4 Kcal/mole, respectively. The results show that the higher the siloxane content, the higher the activation energy for the adhesive bonding process. Also the phase

separation significantly increases the activation energy in comparison between PIS5Si1.1 and PIS5Si2.7, PIS5Si0.6 and PIS9Si0.6. In the SEM mic-rographs, the peeled-off PIS surfaces from the joints show a rougher surface morphology with a higher interfacial adhesion. It is reasonable to surmise that the peel strength of PIS9Si0.6 may be due to the force for plastic deformation because of the relatively smooth peeled-off surface.

Acknowledgments

The authors would like to express their appreciation to the National Science Council of the Republic of China and the China Petroleum Company for financial support for this study under grant NSC 88-CPC-E-009-008. We would like to thank Mr. Able Lee and the Sitron Precision Co., Ltd. for providing the alloy-42 substrate, Dr. Kuen-Ru Juang and High Light Optoelectronic Inc. for providing the d-UV/O_3 source, Mr. Jiin-Peir Jeng for the rheometric dynamic spectrometer measurement, and Mr. Ruey-Tzong Jang for assistance with the peel test.

References

1. L. F. Thompson, C. G. Willson and S. Tagawa, Eds., *Polymers for Microelectronics: Resists and Dielectrics*, Am. Chem. Soc., Washington, DC, 1994, p. 380.
2. M. K. Ghosh and K. L. Mittal, Eds., *Polyimides: Fundamentals and Applications*, New York, Marcel Dekker, 1996, p. 759.
3. P. P. Policastro, J. H. Lupinski and P. K. Hernandez, *Polymeric Materials for Electronics Packaging and Interconnection*, J. H. Lupinski and R. S. Moore, Eds., Am. Chem. Soc., Washington, DC, 1989, p. 140.
4. Y. Okugawa, T. Yoshida, T. Suzuki and H. Nakayoshi, *IEEE*, 570 (1994).
5. E. Sacher, J. E. Klemberg-Sapieha, H. P. Schreiber and M. R. Wertheimer, *J. Appl. Polym. Sci., Appl. Polym. Symp.*, **38**, 163 (1984).
6. L. Ying and R. Edelman, *31st National SAMPE Symp.*, **31**, 1131 (1986).
7. A. K. St. Clair and T. L. St. Clair, *Polyimides: Synthesis, Characterization, and Applications*, K. L. Mittal, Ed., Plenum Press, New York, Vol. **2**, 977 (1984).
8. J. M. Kaltenecker-Commercon, T. C. Ward, A. Gungor and J. E. McGrath, *J. Adhesion*, **44**, 85 (1994).
9. K. Cho, D. Lee, T. O. Ahn, K. H. Sco and H. M. Jeong, *J. Adhesion Sci. Technol.*, **12**, 253 (1998).
10. G. C. Davis, B. A. Heath and G. Gildenblat, *Polyimides: Synthesis, Characterization, and Applications*, K. L. Mittal, Ed., Plenum Press, New York, Vol. **2**, 847 (1984).
11. Y. D. Lee, C. C. Lu and H. R. Lee, *J. Appl. Polym. Sci.*, **41**, 877 (1990).
12. T. Homma, Y. Kutsuzawa, K. Kunimune and Y. Murao, *Thin Solid Films*, **235**, 80 (1993).
13. S. Wu, *Polymer Interface and Adhesion*, Marcel Dekker, New York, 1982, p. 360.
14. L. H. Lee, *J. Polym. Sci., A-2*, **5**, 1103 (1967).
15. J. D. Summers, PhD Dissertation, *Siloxane Modified Engineering Polymers: Synthesis and Characteristics*, Virginia Polytechnic Institute and State University, Blackshurg, VA, 1988.
16. L. P. Buchwalter, *J. Adhesion Sci. Technol.*, **7**, 941 (1993).
17. J. H. Jou, C. H. Liu, J. M. Liu and J. S. King, *J. Appl. Polym. Sci.*, **47**, 1219 (1993).
18. J. Jang and J. H. Lee, *J. Appl. Polym. Sci.*, **62**, 199 (1996).
19. S. P. Kowalczyk, C. D. Dimitrakopoulos and S. E. Molis, *Mater. Res. Soc. Symp. Proc.*, **227**, 55 (1991).
20. A. J. Kinloch, *Adhesion and Adhesives Science and Technology*, Chapman and Hall, New York, 1987, Chapters 2~3.
21. S. L. Jwo, W. T. Whang and W. C. Liaw, *J. Appl. Polym. Sci.*, (accepted, in press).
22. J. S. Riffle, I. Yilgor, A. K. Banthia, C. Tran, G. L. Wilkes and J. E. McGrath, *Epoxy Resin Chemistry* **II**, *ACS Symp.*, R. S. Bauer, Ed., Series **221**, 1983, p. 21.
23. P. J. Andolino-Brandt, C. L. Senger-Elsbernd, N. Patel, G. York and J. E. McGrath, *Polymer*, **31**, 180 (1990).
24. A. R. Gilbert and S. W. Kantor, *J. Polym. Sci.*, **40**, 35 (1959).
25. J. D. Summers, C. S. Elsbernd, P. M. Sormani, P. J. A. Branadt, C. A. Arnold, I. Yilgor, J. S. Riffle, S. Kilic and J. E. McGrath, *Inorganic and Organometallic Polymer, ACS Symp. Series*, M. Zeldin, K. J. Wynne, and H. R. Allcock, Eds., 1988, p. 360.
26. P. V. Wright, *Ring-Opening Polymerization*, K. J. Ivin and T. Seagusa, Eds., Elsevier, New York, Vol. **2**, 1984, p. 1055.
27. W. A. Zisman, *Contact Angle, Wettability, and Adhesion*, F. M. Fowkes, Ed., Washington, D. C., 1964.
28. W. T. Chen and T. F. Flavin, *IBM J. of Res. and Develop.*, **16**, 203 (1972).
29. A. N. Gent and G. R. Hamed, *J. Appl. Polym. Sci.*, **21**, 2817 (1977).
30. K. S. Kim and N. Aravas, *Int. J. Solids Structures*, **24**, 417 (1988).
31. K. S. Kim and J. Kim, *J. Eng. Mater. & Technol.*, **110**, 266 (1988).
32. N. Aravas, K. S. Kim and M. J. Loukis, *Mater. Sci. Eng.*, **A107**, 159 (1989).
33. H. R. Brown and A. C. M. Yang, *J. Adhesion Sci. Technol.*, **6**, 333 (1992).